Monthly Notices
of the
ROYAL ASTRONOMICAL SOCIETY

MNRAS **468,** L16–L20 (2017)
Advance Access publication 2017 February 2

doi:10.1093/mnrasl/slx018

The changing face of α Centauri B: probing plage and stellar activity in K dwarfs

A. P. G. Thompson,[1]★ C. A. Watson,[1] E. J. W. de Mooij[1,2] and D. B. Jess[1]

[1]*Astrophysics Research Centre, School of Mathematics and Physics, Queen's University Belfast, BT7 1NN Belfast, UK*
[2]*School of Physical Sciences, Dublin City University, Glasnevin, Dublin 9, Ireland*

Accepted 2017 January 31. Received 2017 January 31; in original form 2016 November 7

ABSTRACT

Detailed knowledge of stellar activity is crucial for understanding stellar dynamos, as well as pushing exoplanet radial-velocity detection limits towards Earth analogue confirmation. We directly compare archival High Accuracy Radial velocity Planet Searcher spectra taken at the minimum in α Cen B's activity cycle to a high-activity state when clear rotational modulation of $\log R'_{HK}$ is visible. Relative to the inactive spectra, we find a large number of narrow pseudo-emission features in the active spectra with strengths that are rotationally modulated. These features most likely originate from plage, spots or a combination of both. They also display radial velocity variations of $\sim$300 m s^{-1} – consistent with an active region rotating across the stellar surface. Furthermore, we see evidence that some of the lines originating from the 'active immaculate' photosphere appear broader relative to the 'inactive immaculate' case. This may be due to enhanced contributions of, for example, magnetic bright points to these lines, which then causes additional line broadening. More detailed analysis may enable measurements of plage and spot coverage using single spectra in the future.

Key words: techniques: radial velocities – stars: activity – stars: chromospheres – stars: individual: α Centauri B.

1 INTRODUCTION

When trying to take precise radial velocity (RV) measurements of stars, the presence of activity contributes additional 'jitter' to the RV signal, which makes exoplanet detection more difficult. As such, the community makes use of the $\log R'_{HK}$ activity indicator to gauge the detectability of planets and to better constrain RV jitter. This measure, which traces changes of the cores of Ca II H & K, was first done by Wilson (1978), with the long baseline of measurements allowing for activity cycles (similar to the $\sim$11-yr cycle of the Sun) to be mapped for other stars (e.g. Hall, Lockwood & Skiff 2007; Flores et al. 2016, and references therein).

Lovis et al. (2011) looked at stars observed with the High Accuracy Radial velocity Planet Searcher (HARPS) instrument and found that 61 per cent of the 304 FGK stars sampled show periodic variations. They concluded that activity cycles can induce RV variations having a long period and an amplitude up to about 25 m s^{-1}. This result demonstrates the need to better understand the activity of exoplanet host stars, especially when searching for Earth analogues.

Dumusque et al. (2012) studied the RVs of α Cen B (a 5214 $\pm$ 33 K, K1V star) looking for the existence of a planet. They used $\log R'_{HK}$ to get a better handle on the RV jitter, which shows a ramping-up of activity over the course of the observations. The data from the most active nights display a clear periodic variation (see their fig. 2) caused by active regions rotating in and out of view. Although not the main result from the paper, the $\log R'_{HK}$ values show a star going from relatively quiet to active, which provides an interesting test bed to investigate the changes that activity may have on the spectra of K dwarfs.

While the $\log R'_{HK}$ of a star does give an indication of activity, the measure traces changes in the chromosphere. We attempt to better constrain photospheric activity by investigating changes in other spectral lines as a function of $\log R'_{HK}$ activity. In this work, we present results of comparing spectra taken during during high- and low-activity phases of α Cen B. In Section 2, we discuss the data used in this analysis, with more details on the data processing given in Section 2.1. In Section 3, we discuss the changes observed in the generated 'relative' spectra and attempt to model the different morphologies of the observed narrow pseudo-emission peaks. In Section 3.1, we measure the equivalent width of the pseudo-emission features, and finally, in Section 3.2, we look at the radial velocity (RV) shift that these peaks exhibit.

2 DATA

We obtained archival HARPS data of α Cen B from 2008 February to 2011 July as used by Dumusque et al. (2012). These data cover a

★ E-mail: athompson1501@qub.ac.uk

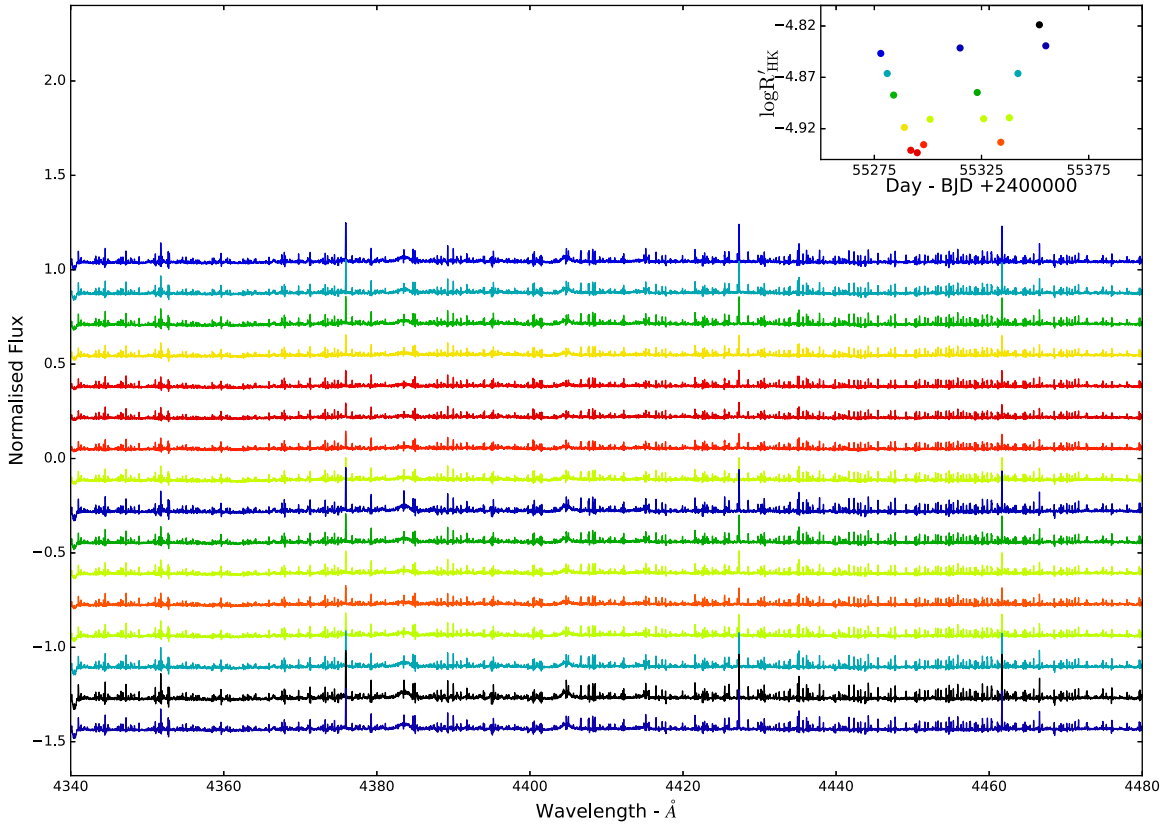

Figure 1. A selection of relative spectra from the 2010 March–June period – generated by dividing high-activity spectra by the master low-activity template – for ease of viewing only 16 of the 48 weighted spectra available for this period are shown. The broad features seen at 4383 and 4404 Å correspond to temperature sensitive Fe I lines. A large number of narrow 'pseudo-emission' peaks can also be seen with the feature at 4375 Å showing an excursion of ∼20 per cent. The colour of the residuals corresponds to the activity as seen in log R'_{HK} (see the inset in the top right-hand panel). Note that the change in the strength of all these features clearly correlates with the rotation cycle of the star.

significant fraction of α Cen B's activity cycle, spanning a range in log R'_{HK} from approximately −5 to −4.82. The full data set consists of 9693 spectra, though in this work we focus our attention on data from 2010 March 23 to 2010 June 12, hereafter referred to as the 2010 March–June period. This range shows a clear rotational variability in log R'_{HK} covering ∼2 of α Cen B's 36.2 d rotation periods (DeWarf, Datin & Guinan 2010). This period is well sampled, with a total of 2475 spectra taken over 48 separate nights.

2.1 Data processing

The spectra were all aligned on to a common wavelength grid, after correcting for the RV shifts as published by Dumusque et al. (2012, including the orbital motion of the binary, light contamination from α Cen A and the barycentric motion of the Earth). The spectra were then all standardized to a common flux level. This was done by dividing each individual spectrum by a high signal-to-noise ratio reference and fitting a fourth-order polynomial to the resulting relative spectrum over the spectral range of 4300 − 5300 Å. Each individual polynomial was then applied to its respective spectrum in order to match their continuum to that of the reference.

For the purposes of this work, we were interested in the difference between high- and low-activity spectra. In order to do this, we identified the night with the lowest stellar activity measure (as defined by log R'_{HK}), which occurred on 2008 February 28. We then stacked all of the data from this night to form a master low-activity template spectrum, after following the process described earlier. In this case, we used the highest signal-to-noise ratio spectrum from 2008 February 28 as the reference in the continuum matching process. The end result was our master low-activity template.

For the 48 nights during the more active 2010 March–June period, we used this master low-activity template as the reference for the continuum matching. For each night, we produce a single nightly spectrum by stacking the continuum matched spectra using a weighted average. The root-mean-square of the relative spectrum (produced by dividing the spectrum by the master low-activity template) was measured in the spectral range of 5050 − 5300 Å and used as the weighting factor. A rejection criterion of greater than 1 per cent in the measured root-mean-squared was included to remove any wrongly labelled α Centauri B spectra (some erroneous observations of α Centauri A took place) or spectra obviously affected by echelle order mismatch.

3 ANALYSIS AND DISCUSSION

Once all of the nightly spectra were created using the process described in Section 2.1, we generated 'relative' spectra by dividing each of the nightly outputs by the master low-activity template. These relative spectra then highlight the differences between the high and low activity of α Cen B.

Visual inspection of the relative spectra for the 2010 March–June period was performed. A representative region (4340–4480 Å) is shown in Fig. 1, which highlights the range of features we observe (to help with observing the changes in the relative features, only 16

of the 48 spectra available are shown in Fig. 1; these 16 are evenly spaced over the period to cover the entire range of log R'_{HK}). Each relative spectrum has been colour coded with respect to its value of log R'_{HK} with an equivalently coloured plot of log R'_{HK} versus time, as shown at the top right-hand side of Fig. 1.

A number of broad features are seen in the relative spectra. Some examples of these can be seen in Fig. 1 at 4383 and 4404 Å, and correspond to Fe I species that are used as spectral-type indicators due to their temperature sensitivity (Giridhar 2010). The broad peak of the Fe I lines indicates a change in temperature of the star. As these lines are known to be photospheric in origin, this temperature change may indicate the presence of cooler active regions (i.e. spots) on the surface of α Cen B.

In contrast, numerous sharp 'pseudo-emission' peaks can be seen; the most prominent in Fig. 1 occur at 4375, 4427 and 4462 Å. The Fe I 4375 Å line, for example, shows a peak at approximately the 20 per cent level, which suggests a significant line change between the high-activity spectrum compared to the master low-activity template. This is similar to the findings of Basri, Wilcots & Stout (1989). However, we note that Basri et al. (1989) constructed similar relative spectra, but used *different* stars to represent high- and low-activity cases. This meant that their results were somewhat inconclusive, as the authors could not be certain that the features they saw were activity driven, or caused by differences in the metallicities, age, $v \sin i$, temperature, surface gravity, etc., between the active and inactive stars – a point raised by Basri et al. (1989) in their analysis.

Since we see morphologically similar results to those reported by Basri et al. (1989) (but without the confusion generated by using different stellar types in the analysis), our work confirms that the bulk of the features reported by Basri et al. (1989) were indeed likely to have been activity driven. The fact that we also see these features modulated on the stellar rotation period of α Cen B further bolsters this conclusion. The features reported are not due to tellurics, as these look distinctly different.

The strength of all the relative features changes alongside the periodic modulation of log R'_{HK}. We investigate this change further in Section 3.1 by measuring the pseudo-equivalent width of the features in the relative spectrum.

The narrow 'pseudo-emission' peaks also show differing profile shapes, as demonstrated in Fig. 2 showing two closely separated lines, Ti II 4443.81 and V I 4444.21 Å. For Ti II 4443.81 Å, we see a distinctive pseudo-absorption trough surrounding the emission peak, which is not present in the neighbouring V I 4444.21 Å line. The stark difference between these two close-by lines also rules out instrumental effects, which would not change so dramatically over this short wavelength range. We have attempted to simulate these two relative line shapes using a simple model that consists of a limb-darkened disc representing the 'immaculate photosphere' and a circular patch at the centre of the stellar disc representing a spotted region. The spotted region covered 4 per cent of the visible modelled stellar surface. We generate Gaussian-shaped line profiles for each point on the star assuming solid body rotation. The line properties (e.g. depth and width) in each region are free parameters in our model. For the immaculate photosphere region, we chose values that best recreated the spectral lines of Ti II 4443.81 and V I 4444.21 Å as seen in the master low-activity template. The depth and width of the line were set to 90 per cent of the continuum and 7.5 km s^{-1}, respectively. For the spotted region, we changed the continuum levels to 10 and 30 per cent that of the immaculate photosphere, which, at the wavelength of the lines, represent a ΔT of ∼1400 and ∼800 K cooler, respectively. The line profiles in the spotted and immaculate photosphere regions were summed together to produce

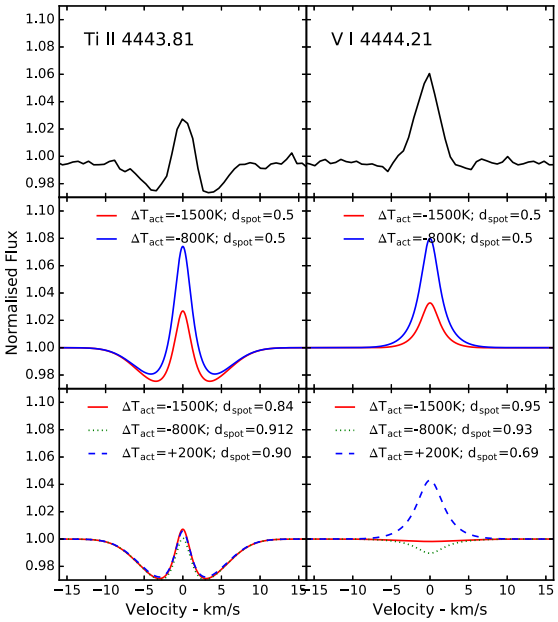

Figure 2. Top panels: two examples of narrow pseudo-emission profiles in the observed relative spectra from closely spaced (∼0.4 Å) and approximately equal strength lines. Both of these profiles show distinctly different morphologies, with the Ti II 4443.8 Å line (left-hand panel) displaying a clear pseudo-absorption trough. Middle panels: We show results for a simple model with a 4 per cent spot feature at disc centre, having a continuum contrast corresponding to a ΔT of ∼1400 and ∼800 K. The line absorption in the spot is ∼50 per cent weaker than the immaculate photosphere. For the left-hand panel, we have assumed that the immaculate line profile in the active spectrum is broadened by 2.5 per cent relative to the inactive immaculate photosphere case – this results in the observed absorption trough. In the right-hand panel, the linewidths in the active and inactive immaculate spectra are identical. Bottom panels: models using the normalized line depth from VALD of the given temperature differences. An additional model of $\Delta T = +200$ K is also shown, which is a proxy for a plage rather than a spotted region.

our high-activity line profile models; a second model disc without a spotted region was generated to model the low-activity line profile. The high-activity line profile was divided by the low-activity one to produce the final relative line profile model for comparison to our data.

As mentioned previously, the Ti II 4443.81 Å line (left-hand plots of Fig. 2) displays a distinctive pseudo-absorption trough. We found that to reproduce this feature changing the parameters of the line profile in the spotted region was not enough. Cegla et al. (2013) show that magnetic bright points (MBPs) can be a source of line broadening (see, for example, their fig. 2); these MBPs exist across the whole surface of the star and are not just constrained to spotted regions. In our model, we broaden the immaculate photosphere (i.e. the non-spotted region) of the active spectrum by 2.5 per cent relative to the inactive immaculate photosphere; this represents the presence of more MBPs across the surface of α Cen B during its more active state. The addition of this term, as well as weakening the absorption strength of the line in the spotted region by ∼50 per cent relative to the immaculate photosphere, allows us to more accurately recover the feature (the middle left-hand panel of Fig. 2). For the V I 4444.21 Å line (right-hand plots of Fig. 2), we did not need to invoke any broadening of the immaculate photosphere to reproduce the feature (shown in the middle right-hand panel of Fig. 2). We then re-ran this model using the Ti II 4443.81

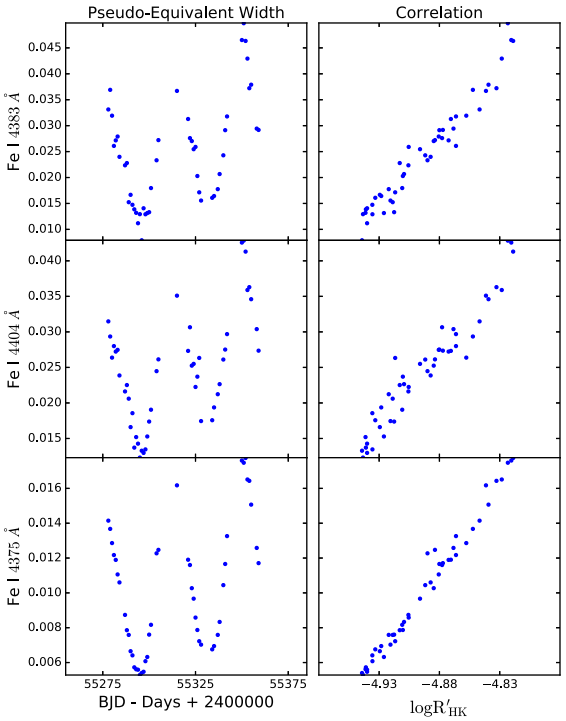

Figure 3. Left-hand panels: the pseudo-equivalent widths of the three lines Fe I 4383 , Fe I 4404 and Fe I 4383 Å plotted against day. Shown are the data during the 2010 March–June period, showing a clear periodic modulation. Right-hand panels: correlation between log R'_{HK} and the same three lines.

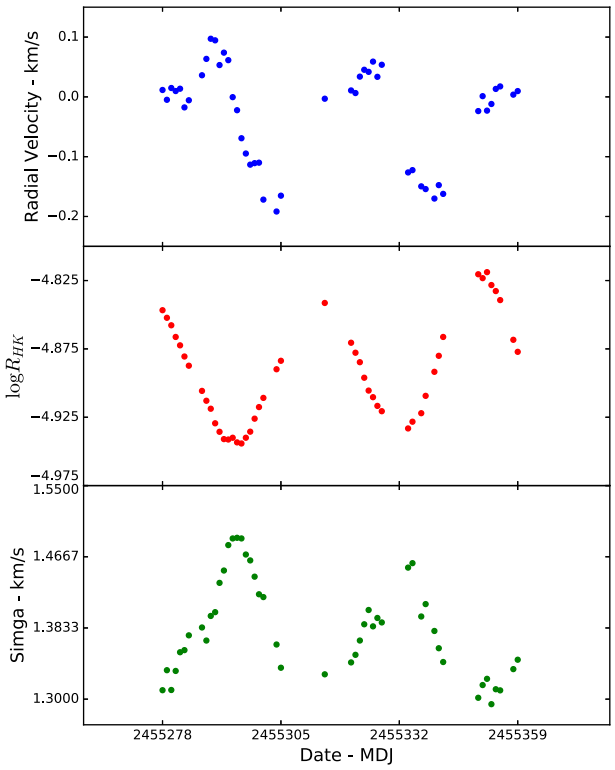

Figure 4. Top panel: the radial velocity measurements, as defined by the peak of the cross-correlation function, for the narrow features in the relative spectra. Middle panel: log R'_{HK} as taken from Dumusque et al. (2012). Bottom panel: the width of the cross-correlation function. Both the top and bottom plots show, with varying degrees of phase lag, the same period variation as seen in log R'_{HK}.

and V I 4444.21 Å lines depths given by VALD (Vienna Atomic Line Database, Ryabchikova et al. 2015) for spot temperatures with ΔT of ∼1400 and ∼800 K. These models (bottom panels, Fig. 2) show that, while we can still reproduce the overall morphology of the Ti II 4443.81 line, we cannot reproduce the V I 4444.21 Å line assuming a simple cool spot model. To explore this further, we generated a model assuming that the spotted region was 200 K hotter that the immaculate photosphere as a proxy for a hotter plage region. This gives a qualitatively better fit to the observed V I 4444.21 Å line feature, and demonstrates the complexity of modelling these lines.

The differing morphologies also imply a difference in the physical processes that affect the line strength during changes in activity, with some lines being more affected by magnetic activity than others. We believe that using such lines in high-precision RV measurements could increase RV noise, which could be mitigated by looking only at lines with weak (or no) sensitivity to stellar activity.

3.1 Iron line pseudo-equivalent width

The peaks in the relative spectra shown in Fig. 1 display a correlation with log R'_{HK}. We calculate the pseudo-equivalent width of three close-by features in the relative spectra: Fe I 4383 , Fe I 4404 and Fe I 4375 Åin order to better trace the changing strength of the lines. The pseudo-equivalent width was taken as the area of a Gaussian fit to each of the features. The Fe I 4375 Å line is a narrow feature that does not show any pseudo-absorption trough, while the other two show broad features in the relative spectrum. In Fig. 3, we show how the strengths of the three pseudo-equivalent widths respond to changing levels of activity (as indicated by log R'_{HK}) for the 2010 March–June period. This period is characterized by a rotational modulation of log R'_{HK}, and a similar variation is observed in all three lines. This adds validity to the argument that the features are real, as producing such a correlation by data processing or instrumental effects would be very difficult.

For the three lines, a clear periodic modulation of their pseudo-equivalent width matches the rotational period of α Cen B. The relative strengths of each of the Fe I lines are plotted against night (left-hand panels of Fig. 3); this suggests that the changing strength of the features is due to active regions rotating across the surface of the star. The correlation of the pseudo-equivalent widths against log R'_{HK} is also shown in the right-hand panels of Fig. 3, with all pseudo-equivalent widths having a Pearson R value of >0.96.

This result more rigorously demonstrates the changes observed in Fig. 1, and shows that the changing strength of both the broad and narrow features mimics the rotational variation seen in the value of log R'_{HK}.

3.2 Radial velocity variations

If the features are activity driven, the position of the peak centre should vary over the course of the rotation period. To test this, we selected the first night in the 2010 March–June period and fit Gaussians to all peaks in the relative spectrum that were stronger than 5 per cent. A template was generated from this fit, which was then cross-correlated with each of the relative spectra in the 2010 March–June period.

We measured the velocity change of the relative peaks and found that the lines show a peak-to-peak velocity change of ∼300 m s^{-1} (top panel in Fig. 4). Compared to log R'_{HK} (middle panel of Fig. 4),

the RVs of the pseudo-emission peaks show a phase difference of approximately 90°. This can be understood by considering a rotating active region. At the disc centre, $\log R'_{HK}$ is at maximum as the active region has maximum visibility; however, the RV of the active region will be at $0\,\mathrm{km\,s^{-1}}$ (relative to the systemic velocity of the system). As the feature rotates out of view towards the stellar limb, foreshortening will decrease $\log R'_{HK}$, and the feature will become progressively redshifted. Conversely, the opposite trend occurs as the feature rotates back into view. This is akin to the motion of apparent emission bumps due to spots through stellar line-profiles, typically associated with more rapidly rotating stars suitable for Doppler imaging (Vogt & Penrod 1983; Collier Cameron & Donati 2002).

The width of the cross-correlation functions (CCFs) is shown in the bottom panel of Fig. 4. These are anticorrelated with $\log R'_{HK}$, with the CCFs broadest when $\log R'_{HK}$ is lowest. This suggests that active regions are more homogeneously distributed across the stellar surface during times when the main active region has rotated out of direct view. The narrow CCF widths at high $\log R'_{HK}$ then lend support for the presence of a localized highly active region (and hence spanning a limited range in stellar surface velocities). Of course, this is likely to be a simplistic picture due to the probable presence of several active regions. The effects of plage and MBPs would also need to be considered as they have been shown earlier in Section 3 to cause pseudo-emission peaks of very different morphologies and may need to be considered separately in our cross-correlation analyses. As such, more in-depth analysis of the effects of plage on relative peak morphology and spots on the temperature sensitivity of the broad relative peaks of the the Fe I species is needed to better constrain the effects reported here.

4 CONCLUSIONS

We investigate the effects that stellar activity has on the spectrum of α Cen B. We present evidence that the strength of a large number of spectral lines changes due to the effects of active regions rotating in and out of view. Relative spectra – created by taking high-activity spectra and dividing them by a master low-activity template – show distinct narrow and broad features. These features have strengths and radial velocities that are modulated on the rotation period of the star, and we show that they are associated with stellar activity.

The narrow peaks show differing morphologies, the most prominent being pseudo-emission lines superimposed on top of broader absorption troughs. We demonstrate that this can be explained if absorption lines from the 'active immaculate' photosphere are broader than their 'inactive immaculate' photosphere counterparts. We suggest that this could arise due to a higher filling factor of MBPs during the active phases, which may lead to a general enhanced line-broadening across the stellar photosphere relative to the inactive case. In addition, broad features seen at Fe I 4383 and Fe I 4404 Å in the relative spectra belong to temperature-sensitive Fe I lines, suggesting a change in the surface temperature of α Cen B (leading to an apparent change in spectral type).

This work demonstrates the need to better understand the nature and effects that activity and rotating active regions can have on the measurement of spectral lines. In particular, the evidence that some strong lines can show distinct changes between the active and inactive states, while other similarly strong lines do not show such pronounced differences, suggests the ability to pre-select well-behaved lines suitable for high-RV-precision work. This will be explored in more detail in a future paper. As we move closer to the launch of missions dedicated to the discovery of Earth-analogue planets (such as PLATO), such work may become critical in the RV confirmation of small, terrestrial planets. In order to provide line-lists of stellar-activity insensitive lines as a function of spectral type, we would urge the community to begin monitoring stellar activity cycles of likely mission targets such that bespoke low-activity comparison spectra may be obtained.

ACKNOWLEDGEMENTS

APGT acknowledges funding from the Northern Ireland Department of Eduaction, and EJWdM would like to acknowledge the support of the Michael West Fellowship. CAW acknowledges support from STFC grant ST/L000709/1. This work has made use of the VALD data base, operated at Uppsala University, the Institute of Astronomy of RAS in Moscow and the University of Vienna. We would like to thank the anonymous referee for useful comments on this Letter.

REFERENCES

Basri G., Wilcots E., Stout N., 1989, PASP, 101, 528
Cegla H. M., Shelyag S., Watson C. A., Mathioudakis M., 2013, ApJ, 763, 95
Collier Cameron A., Donati J.-F., 2002, MNRAS, 329, L23
DeWarf L. E., Datin K. M., Guinan E. F., 2010, ApJ, 722, 343
Dumusque X. et al., 2012, Nature, 491, 207
Flores M., González J. F., Jaque Arancibia M., Buccino A., Saffe C., 2016, A&A, 589, A135
Giridhar S., 2010, Bull. Astron. Soc. India, 38, 1
Hall J. C., Lockwood G. W., Skiff B. A., 2007, AJ, 133, 862
Lovis C. et al., 2011, preprint (arXiv:1107.5325)
Ryabchikova T., Piskunov N., Kurucz R. L., Stempels H. C., Heiter U., Pakhomov Y., Barklem P. S., 2015, Phys. Scr., 90, 054005
Vogt S. S., Penrod G. D., 1983, PASP, 95, 565
Wilson O. C., 1978, ApJ, 226, 379

This paper has been typeset from a TEX/LATEX file prepared by the author.